Impact of the contacting scheme on I-V measurements of metallization-free silicon Heterojunction solar cells

Malte Brinkmann^{1,2}, Felix Haase¹, Karsten Bothe¹, Karsten Bittkau², Andreas Lambertz², Weiyuan Duan², Kaining Ding², Hans-Peter Sperlich³, Andreas Waltinger³, and Henning Schulte-Huxel¹

Short Title: Contacting of metallization-free HJT cells for I-V measurements

Abstract

I-V measurements are sensitive to the number and positioning of current and voltage sensing contacts. For busbarless solar cells, measurement setups with contact wires have been developed using separate voltage sense contacts. Placing the latter at a defined position allows a grid resistance neglecting measurement and thus I-V characteristics independent from the contacting system. This technique has been developed for solar cells having a finger grid and thus good lateral conductivity. The optimal position of the sense contact in case of finger-free silicon heterojunction solar cells has not yet been studied. Here, the lateral charge carrier transport occurs in a transparent conductive oxide layer resulting in a higher lateral resistance. We investigate its impact on the grid resistance neglecting measurement method by performing finite different method simulations of HJT solar cells without front metallization. We present fill factor measurements of metal free solar cells with varying TCO sheet resistances measured using two types of contacting schemes. By correcting for the voltage sense contact position using the simulation results, we can reduce the difference in FF measurements between the two setups from 8.5% to below 1%, with both values within their respective confidence intervals.

Keywords: heterojunction solar cell/i-v measurement/contacting/fill factor/metal-grid free

1 Introduction

The high efficiency and bifaciality of silicon heterojunction solar cells (HJT) as well as their lean process flow results in an increased production capacity of this cell technology since the mid 2010s, although the average cost per module is still higher than most other technologies [1]. A high portion

of the costs can be assigned to the silver consumption for the metallization on both sides of HJT cells using low-temperature silver pastes also suffering from reduced conductivity compared to Ag pastes processed at high temperatures [2, 3]. Therefore, reducing the amount of silver used for HJT solar cells and in the photovoltaic sector overall is

 $^{^1\}mathrm{Institute}$ for Solar Energy Research Hamelin, Am Ohrberg 1, 31860 Emmerthal, Germany

²Leibniz University of Hanover, Institute for Solid State Physics, Appelstraße 2, 30167 Hannover, Germany

³Institute of Energy and Climate Research 5 – Photovoltaic, Research Center Juelich, 52425 Juelich, Germany

⁴Meyer Burger GmbH, An der Baumschule 6-8, 09337 Hohenstein-Ernstthal, Germany

a major goal in recent solar cell research [4]. The transparent conductive oxide (TCO) on the surface of heterojunction solar cells in principle enables an operation without any metallization on cell level [5, 6]. The lateral charge carrier transport then occurs primarily in the TCO, but with a much higher series resistance compared to a metal grid. For module integration the cell interconnectors are directly contacted to the TCO. This is also of high interest for perovskite/c-Si tandem solar cells featuring in general a TCO layer but having high requirements towards the metallization process [7].

Measuring the current-voltage (I-V) characteristics of bare solar cells is crucial to compare cells and cell processes. While many aspects of the measurement conditions are standardized there is no international standard on the non-permanent and non-destructive contacting of the cells. It has been shown that the I-V characteristics, especially the fill factor (FF) and efficiency highly depend on the contacting procedure [8]. Typically, separate contacts for current extraction and voltage sensing are used to ensure a four probe configuration and an independent measurement of the voltage and current characteristics.

For solar cells with busbars (BB) an infinite number of current points is used to contact the cell resulting in a busbar-resistance neglecting (brn) I-V characteristic [9]. Having only a finite number of contacts leads to a voltage drop between two current extraction points due to the non-zero resistivity of the busbar. Using a smart positioning of the voltage sense contact allows to approximate the infinite number of current contacts and to measure the average voltage over the busbar [10].

Going from solar cells with busbars to busbarless cells there are at least two different approaches to contact these cells using either contacting bars or wires stretched over a slightly bent solar cell contacting all fingers of the cell. Comparable to the contacting of cells with busbar using a finite number of contacts the resistivity of the fingers result in a voltage drop between two current contacts. The gradient and height of this drop depends on the number of current contacts, and the resistivity of the finger leading to a dependency of the measured voltage on the position the voltage sense contact.

Different approaches can be found in the literature on how to electrically contact bare solar cells. Some prefer a contacting comparable to the integration in the module [11, 12]. The so-called grid-resistance-including (gri), places the voltage sense contact in proximity to the current contacts representing the cell performance in a module [9]. Here, the measured fill factor and efficiency depend on the number of current contacts and the resistivity of the metal grid and measurements of two different systems can not be easily compared.

Widely accepted is the approach to measure solar cells independently from the contacting procedure resulting in comparable measurement between different systems [10, 13, 14]. For this second approach a smart sensing concept is used to approximate the contacting of the full metal grid resulting in a measurement independent from the contacting system and the resistivity of the metal grid [14]. Here, the voltage sense contact is placed between two current extraction wires. Bothe et al. showed, for a sufficiently high number of current wires, that the full contacting can be approximated by placing the sense contact at the same relative position between two current contacts independently of the actual amount of current wires. This approach is called the *grid-resistance neglecting* (*grn*) method. They also showed the dependency on the specific resistivity of the metal grid. Measuring the fill factor is highly sensitive to even small deviation from the ideal sense position and this sensitivity increases with rising finger line resistivity.

Now, omitting the metallization of heterojunction solar cells completely leads to a high increase in series resistance because the charge carrier transport occurs primarily in the TCO. Therefore, special care has to be taken for the non-permanent and non-destructive electrical contacting to measure the I-V characteristics of the cells before module integration.

In this paper we simulate the I-V measurement of HJT solar cells without metallization to test for the approximation for solar cells with finger metallization but without busbars made by Bothe et al. which allows to measure the same I-V results independently from the contacting. The I-V curve at several positions of the voltage sense contact between two current extraction wires/bars is simulated for various sheet resistances of the front TCO and number of wires used for contacting. The corresponding fill factors are extracted and compared against the quasi full contacting case with an equipotential voltage over the whole cell area to find the position of the sense contact for the grn measurement of each parameter. The simulations are then compared to I-V measurements of different cells with various sheet resistances. The measurements are performed with two different measurement systems. We show the high dependency of fill factor and efficiency measurements on the position of the voltage sense contact for solar cells with high lateral resistance. Later, we discuss appropriate measurement procedures for such cells.

2 Methods

2.1 Simulations

We simulate the measurement of HJT solar cells without metallization to find the optimal positioning of the voltage sense contact with the commercially available tool *Quokka3* using finite different method (FDM) simulations. For various sheet re-

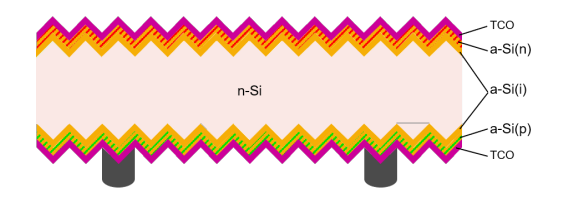


Figure 1: Schematic cross section of the simulated HJT solar cell without front metallization.

sistances of the TCO as well as different wire/bar configurations of the contacting setup we simulate the I-V curve of the respective cell.

A schematic cross section of the simulated cell is shown in Figure 1. The bulk is covered on both sides with a skin layer where the amorphous layers are combined with the TCO with respective sheet resistances. To simulate the electrical effects only, the skin layers are set to be fully transparent. The front side is contacted by structures representing the current extraction wires with neglected contact resistance. The fingers on the rear side of the cell are contacted by a full area contact.

Figure 2 shows the schematic top view of the solar cell, here connected by 12 wires for I-V measurements including the voltage sense contacts positioned in proximity to one of the wires/bars. For the FEM simulations the cell is divided into an unit cell which is periodic in both x- and y-direction (see magnified part). Pads (dark yellow) are positioned on two sides of the unit cell for contacting. They are chosen to be transparent to prevent an influence on $I_{\rm sc}$ and $V_{\rm oc}$.

While Bothe et al. showed the voltage distribution under maximum power point conditions only this is not sufficient when going to higher lateral resistivities. In Figure 3 the current-voltage and power-voltage curves for sheet resistances of $1\,\Omega/\text{sq}$, and $200\,\Omega/\text{sq}$, are plotted for a contacting unit using 12 wires but different relative positions of the voltage sense contact d_{sp} of 0 (at the current contact), 0.2 and 0.5. Since the open circuit voltage and short circuit

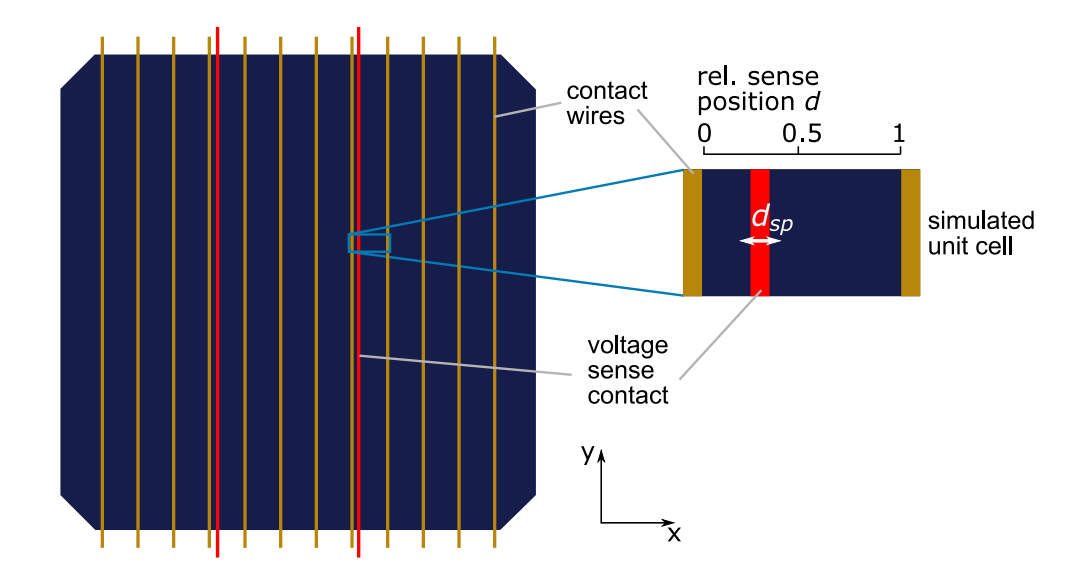


Figure 2: Schematic top view of measurement setup with 12 contact wires/bars including two sensing contacts for precise voltage measurements. The magnification shows the unit cell used for the simulations.

voltage are set to be similar for all cells, the curves are only shown around the maximum power point. The curves and thus the maximum power points differ significantly from each other for high sheet resistances when placing the position of the sense contact at different positions. Therefore, we extract the $V_{\rm MPP}$ and $J_{\rm MPP}$ to calculate the

fill factor for each position of the voltage sense contact d_{sp} . The resulting fill factor distribution over the position of the voltage sense contact is then compared to the equipotential voltage distribution resulting from a full contacting of the cell. The latter is achieved by adding a transparent pad over the complete unit cell. Finding

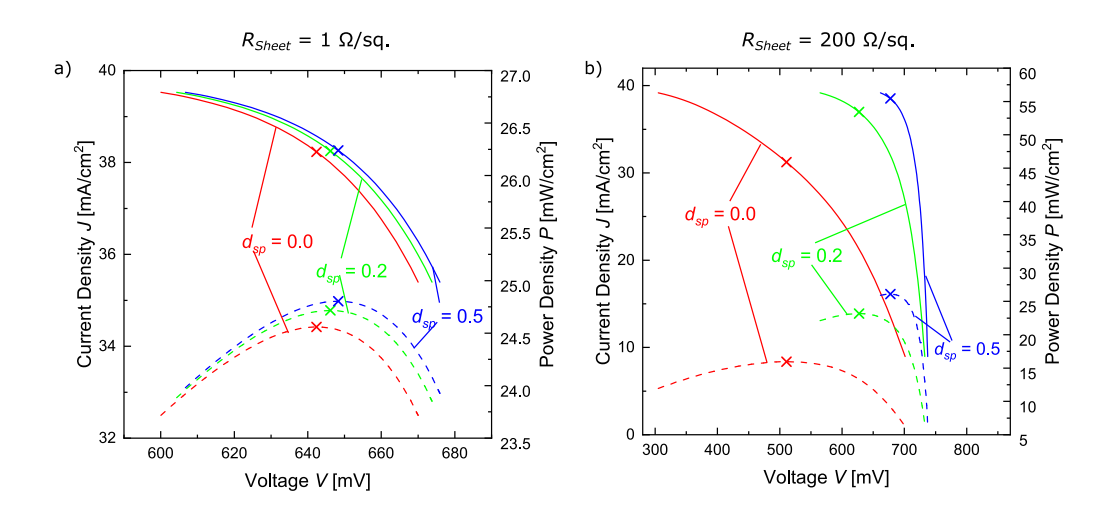


Figure 3: I-V (compact line) and P-V (dashed line) curves around the maximum power point of HJT solar cells with sheet resistances of a) $1 \Omega/\text{sq}$, and b) $200 \Omega/\text{sq}$, for different positions of the voltage sense contact d_{sp} using a contacting unit consisting of 12 current wires. The respective MPPs are depicted as crosses.

the intersect between these distributions and placing the voltage sense contact there allows to measure the fill factor of these cells neglecting the lateral resistance.

2.2 Measurements

To verify our simulations, we measure three HJT cells with various oxygen content in indium tin oxide resulting in different sheet resistances of the TCO in two measurement systems with different contacting frames. The first system (abbr. as LOANA) manufactured by pv-tools consists of 12 contacting bars with two voltage sense contacts. The second one from Pasan SA uses 30 wires over a bended surface to contact a solar cell with 5 additional voltage sense contacts (abbr. as PASAN). For both systems the reproducibility of the measured FF is better than $0.1\%_{abs}$ when contacting the cell several times. To verify the comparability of the two systems we also characterized fully metallized HJT solar cells with both measurement systems. We found an agreement of the measured open circuit voltage, short circuit current, fill factor and efficiency within $1\%_{abs}$ of all values.

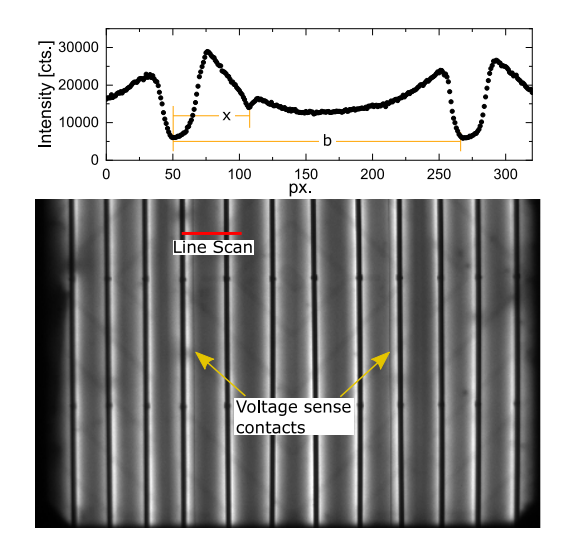


Figure 2: EL Picture of a HJT solar cell without front metallization contact with 12 bars and 2 voltage sense contacts.

The positions of the voltage sense contacts are determined from electroluminescence (EL) pictures by using a linescan over the 2 bars with a sense contact in between (see Figure 2). By measuring the distance between two current bars b and the distance between one current bar and the voltage sense contact x we calculate the relative position of the voltage sense contact between the two current bars. The precision of this methods depends on the resolution of the EL image which is 16 px/cm for the LOANA system and $6.4 \,\mathrm{px/cm}$ for the PASAN measurement system. The average relative position of each sense contacts of the LOANA is 0.20 ± 0.02 between the current extraction wires/bars and 0.35 ± 0.10 for the PASAN Spotlight system. Both uncertainties are dominated by the resolution of the EL images.

3 Results

3.1 Simulations

We simulate the fill factor distribution of solar cells with TCO sheet resistances ($R_{\rm Sheet}$) between $1\Omega/{\rm sq}$, to $200\,\Omega/{\rm sq}$, and for different number of wires between 12 and 35 distributed equidistantly over the cell area. While $1\,\Omega/{\rm sq}$, is an optimistic assumption for a TCO, it has been shown to be achievable with low losses in transparency [15].

The resulting fill factor distributions is plotted over the relative position of the voltage sense contact d_{sp} between two adjacent current wires/bars in Figure 4, exemplary for sheet resistances of the TCO of $1\Omega/\text{sq.}$, $50\Omega/\text{sq.}$ and $100\Omega/\text{sq.}$. The approximately parabolic distributions are symmetric around the middle of the current wires. Therefore, the voltage is only plotted in the range from $d_sp=0$ to 0.5. Additionally, the equipotential voltage of the fully contacting cell is plotted. For a small sheet resistance of $1\Omega/\text{sq.}$ the distributions of all number of wired intersect

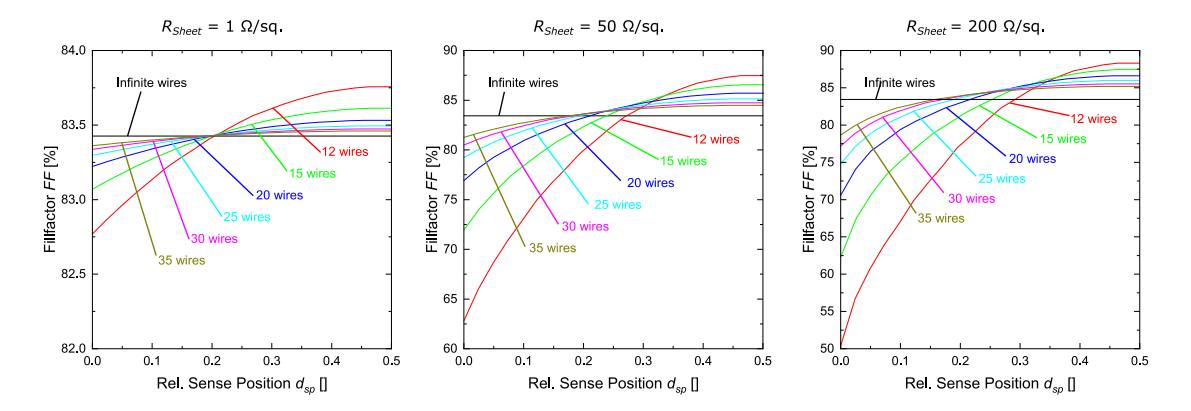


Figure 4: Fill factor distribution between two current wires at MPP conditions for a HJT solar cell with $R_{\text{Sheet}} = 1 \,\Omega/\text{sq.}$, $50 \,\Omega/\text{sq.}$ and $200 \,\Omega/\text{sq.}$.

the fill factor achieved by a full contacting of the metal grid. For a cell with very low sheet resistances a grn measurement is still possible when placing the sense contact at $d_{idsp} = 0.2$.

This dependency does not hold with rising sheet resistances. The fill factor distributions shown in Figure 4b) and c) don't cross the black line representing the fully contacted cell at a specific position. For 12 and 15 wires the sense position for a grid resistance neglecting measurement shifts closer to the middle between two current wires resulting in a underestimation of the fill factor when sensing the voltage at $d_{idsp} = 0.2$. Measuring a cell with a TCO sheet resistance of $200 \Omega/\text{sq}$. leads to a FF which is 7% lower than the FF neglecting the lateral resistance. Using 20 and more wires this trend is opposing and the fill factor will be overestimated for voltage sense position at $d_{idsp} = 0.2$. Contacting a $200 \Omega/\text{sq.}$ cell with 35 wires and sensing the voltage at d_{idsp} results in an overestimation of 0.8%.

Similar simulations for the other TCO sheet resistances are used to identify the optimal sense contact positions summarized in Figure 5a). For small sheet resistances it is at 0.2 nearly independently from number of wires. Going to higher sheet resistances the position of the voltage sense for a grid resistance neglecting measurement shifts. Us-

ing a low amount of wires results in shift of the sense contact towards the middle of the current wires converging at 0.28 for 12 wires and 0.25 for 15 wires. The large voltage drop between two adjacent current wires results in different operating points of the cell depending on the distance to the current wires which are different from the maximum power point. Not only $V_{\rm MPP}$ changes but also $J_{\rm MPP}$ is considerably different.

On the other hand, using more wires results in a shift of the voltage sense position for the grid resistance neglecting measurement closer to one of the current wires. The lower voltage gradient between two adjacent wires allows similar operating points over the whole cell and the fill factor distributions follow the voltage distribution showing the same behaviour.

There seems to be an ideal number of wires of 23 corresponding to a distance between two current wires of 4.5 mm resulting in the same position of the voltage sense contact for a grid resistance free measurement independent of the TCO sheet resistance. While this might be true for the specific cell parameters we simulated here we were can not confirm this for solar cells with different properties at the moment.

Additionally, we investigate the error in fill factor measurements when placing the sense contact placed at a fixed position of 0.2, so the ideal position for metallized cells

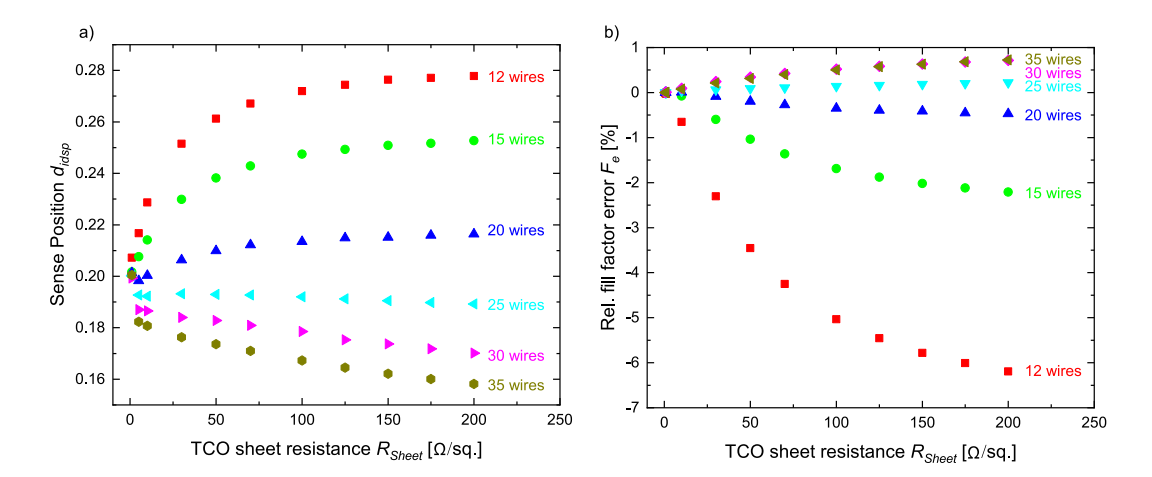


Figure 5: a): Simulated relative position of the voltage sense contact where V_{MPP} -measurement is free of lateral resistance for varying TCO sheet resistances. b): Error in FF measurement when placing the sense contact at $d_{sp} = 0.2$ depending on number of wires used for contacting and sheet resistance of TCO.

and cells with small resistivity. Figure 5b) shows that using only 12 wires the error is up to $6.2\,\%_{\rm rel}$ ($5.2\,\%_{\rm abs}$) for cells with a sheet resistivity of $200\,\Omega/{\rm sq.}$. For 30 or 35 wires the error is considerably smaller with an overestimation of the FF up to $0.7\,\%_{\rm rel}$ ($0.6\,\%_{\rm abs}$) allowing for a much improved accuracy of the I-V measurement. The measurements are most robust regarding the TCO sheet resistance when using 25 wires with error in the fill factor measurement of $0.2\,\%_{\rm rel}$ ($0.17\,\%_{\rm abs}$) due to non ideal placing of the voltage sense contact.

The fill factor distributions in Figure 4 show rising gradients for fewer wires (and thus greater distance between the wires). Therefore, we analyse the simulations regarding the uncertainty of the positioning of the voltage sense contact and the resulting uncertainty in FF measurements (see Figure 6). Assuming a placement accuracy for the voltage sense contact of $\pm 0.25 \,\mathrm{mm}$, which is the case for the LOANA system, the FF can be overestimated up to $1.0\%_{\rm rel}$ $(0.8\%_{abs})$ for contacting geometries with a low amount of contacting bars/wires. On the other hand, if the sense is to close to the current extraction wire, the FF is underestimated up to $1.2\%_{\rm rel}(1.0\%_{\rm abs})$. The asymmetry of the over- and underestimation of the FF is caused by the increasing gradient of the fill factor distributions with decreasing distance of the sense contact to the current wires. A contacting unit with 35 wires has an ideal sense position shifted closer to smaller relative sense positions

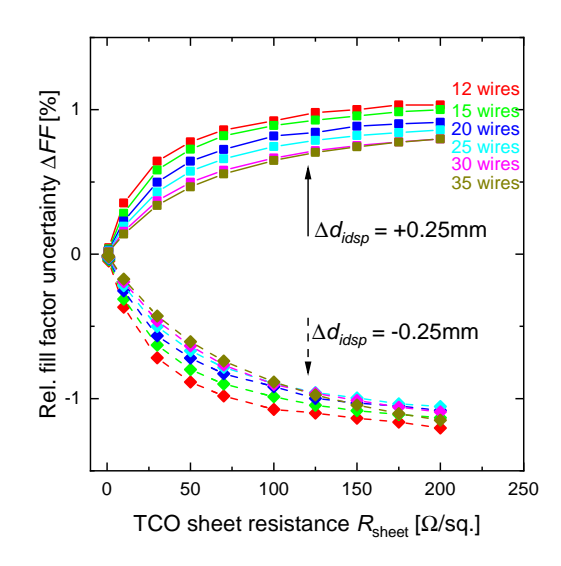


Figure 6: Rel. uncertainty in FF -measurement due to a misplacement of $-0.25\,\mathrm{mm}$ (diamonds, dashed line) and $+0.25\,\mathrm{mm}$ (squares, compact line) of the voltage sense contact depending on R_{Sheet} of the TCO for different wire/bar distances.

with rising sheet resistances resulting in an higher uncertainty of the FF measurement compared to a contacting with less wires.

For rising $R_{\rm Sheet}$ of the TCO contacting systems with a larger number of wires are more robust due to the smaller gradient of the fill factor distribution. Nevertheless, the measurements are very sensible to the position of the voltage sense contact. To measure the FF of a solar cell having TCO sheet resistances up to $200\,\Omega/{\rm sq}$, with an uncertainty smaller than $1\,\%_{\rm rel}$ using a contacting unit consisting of 30 wires, the sense contact has to be positioned with an accuracy of $0.25\,{\rm mm}$ or better.

3.2 Measurements

The FF-measurements of three solar cells without a metallized front side and different TCO sheet resistances of 72, 123 and 175 Ω /sq. are compared to validate the simulations. The pseudo fill factor of these cells is nearly the same with 85.2, 85.6 and 85.3 %, respectively.

For the three different cells, the voltage

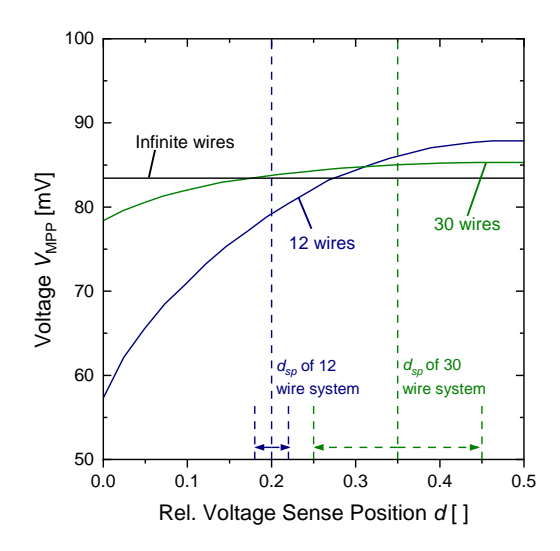


Figure 7: Simulated fill factor distribution of a HJT cell without front metallization and $R_{\text{Sheet}} = 123 \,\Omega/\text{sq}$. compared against fill factor of a fully contacted cell. The uncertainty of the voltage sense position is illustrated at the bottom.

sense contact would be ideally positioned at 0.265 (0.181), 0.273 (0.175) and 0.277 (0.171) for the LOANA (PASAN) system, respectively (see Figure 5a)). The non-ideal placement of the voltage sense contacts of 0.2 for the LOANA and 0.35 of the PASAN system (see subsection 2.2) results in larger differences between the measured FF of the two systems the higher the sheet resistance of the TCO. For $R_{\rm Sheet} = 175\,\Omega/{\rm sq}$, the discrepancy in FF is up to 8.75 %_{abs} as shown in Figure 8a).

By using our simulations, we can estimate the influence of non-ideal positioning of the voltage sense contact. In Figure 7 the voltage distribution between adjacent current contacts of the cell with a sheet resistance of $123 \Omega/\text{sq}$. is shown for the contacting units of the two measurement systems and compared to the voltage of a fully contacted cell at the sense respective positions d_{sp} . We extract the overestimation of the fill factor measurement and add the difference to the measured fill factors resulting in a corrected FF were the non-ideal position of the voltage sense contact is compensated. The correction values $\Delta_{FF}(\text{LOANA})$ and Δ_{FF} (PASAN) for the two contacting units are summarized in Table 1.

Correcting the measured FF with these values we are able to reduce the maximum difference between the two measurement setups to below $1\%_{abs}$. The uncertainty range in Figure 8b) indicate the additional uncertainty due to the positioning precision

$R_{\mathrm{Sheet}} \left[\Omega / \mathrm{sq.} \right]$	$\Delta_{FF}(\mathrm{LOANA})$	$\Delta_{FF}({\rm PASAN})$
72	+4.5	-1.3
123	+5.7	-1.6
175	+6.3	-1.8

Table 1: Correction values for the FF to compensate for the non-ideal position of the voltage sense contact for the two used contacting units.

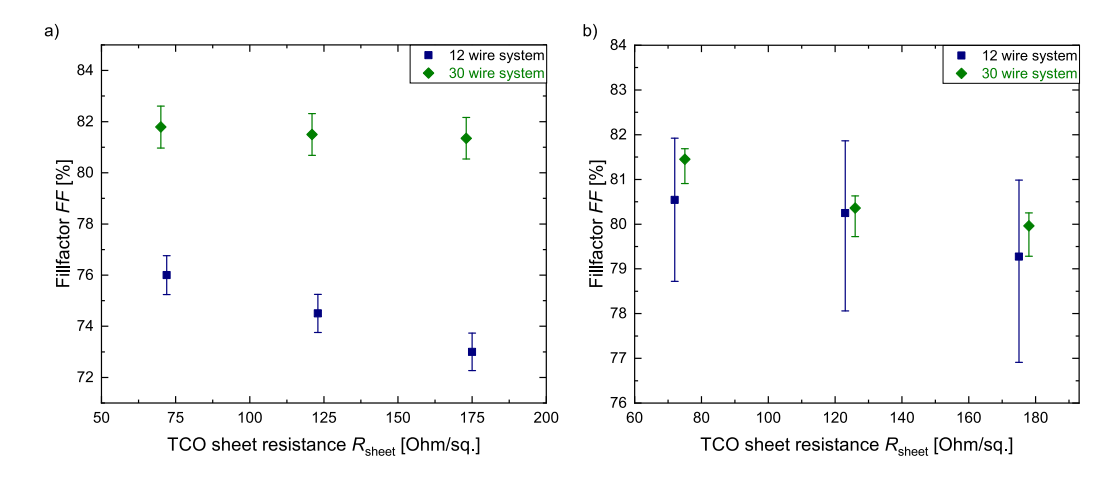


Figure 8: Measured FF of 3 cells with different TCO sheet resistance for two different setups (blue: 12 wires, rel. sense position = 0.2; green: 30 wires, rel. sense position = 0.35). In a) the directly measured values are shown. In b) the FF of the same measurement setup and cells but with corrected values for the misplaced voltage sense contact is plotted.

of the voltage sense contact determined from EL pictures (see subsection 2.2). In Figure 7 the uncertainty of the voltage sense position d_{sp} is shown. Due to the higher gradient of the voltage distribution for the contacting unit with 12 wires the uncertainty is higher for this system. The proposed post-processing of the measurements allows reconstructing of a grid resistance neglecting measurement of HJT solar cells without front metallization with two different measurement systems.

4 Discussion

Going towards solar cells without front metallization poses new challenges on the accurate measurement setups of solar cells. The grid-resistance neglecting contacting concept for metallization-free HJT cells requires precise positioning of the voltage sense contact. Also, when measuring cells with different sheet resistances of the TCO the voltage sense contact has to be repositioned. On the other hand, it is plausible to place the voltage sense at a fixed position and to compensate the FF and efficiency measurements afterwards with simulation comparable to those presented in this pa-

per. This requires a precise knowledge of the cell for an accurate representation in the simulation.

Nevertheless, as shown in Figure 4, the voltage at the current extraction rods, so a relative position of the voltage sense d=0, is considerably lower than the equipotential voltage distribution. In a PV module only the voltage at the wire can actually be utilized. Therefore, for HJT solar cells without metallization a grid-resistance including contacting scheme seems to be more suitable. Placing the voltage sense contact very closely to the current extraction wire gives a more realistic representation of the cell performance in the module.

For the integration of metal-free heterojunction solar cells without metallization into modules low sheet resistance of the TCOs are necessary to reduce series resistance losses. On the other hand, reducing $R_{\rm Sheet}$ is typically achieved by a lower oxygen doping of the TCO resulting in less transmission hence lower current generation. We estimate sheet resistance between $50\,\Omega/{\rm sq.}$ and $100\,\Omega/{\rm sq.}$ to have a suitable properties for module operation. Here, we estimate 25 to 30 wires for the interconnection of cells with M6 wafer size to achieve a

performance with a fill factor in the range of 80% on module level.

5 Conclusion/Summary

We perform FDM simulations to test the approximation of Bothe et al. made for the positioning of the voltage sense contact of busbarless solar cells during I-V measurements for HJT solar cells without front metallization. The voltage distribution between two contact wires/ bars is simulated for various sheet resistances of the front TCO. We can confirm the results of Bothe et al. with our simulations for small sheet resistances. Going towards higher sheet resistances of metallization free HJT solar cells the optimal relative position of the voltage sense contact becomes dependent of the sheet resistance of the TCO and the number of wires used for contacting. Simulating different wire distances, we observe high sensitivity of fill factor measurements to the positioning of the voltage sense contact. Misplacing the voltage sense contact by $\pm 0.25 \,\mathrm{mm}$ leads to an uncertainty in FFmeasurement of up to $1.2\%_{\rm rel}$, depending on the sheet resistance of the TCO and wire geometry. Estimating the resulting errors in FF-measurements due to the uncertainty in positioning the sense contact gives a precision requirement for $\Delta FF < 1\%_{\rm rel}$ of the voltage sense contact to 0.25 mm for 30 contacting wires and TCO sheet resistances up to $200 \Omega/\text{sq.}$.

We measure HJT cells without front metallization with varying sheet resistances with two different measurement systems using 12 (2) bars and 30 (5) wires for current extraction (voltage sensing). By correcting for the voltage sense contact position using the simulation results, we can reduce the difference in FF-measurements between the two setups from 8.75% to below 1%, with both values within their respective confidence range.

Acknowledgments

This work was financially supported by the German Federal Ministry for Economic Affairs and Climate Action (BMWK) under contact number 03EE1080C (TOP). The authors thank J. Hensen, M. Wolf and D. Sylla (all ISFH) for their contribution to the measurements of the metallization-free solar cells.

References

- 1. PV Infolink, New Technology Market Report 2021.
- 2. VDMA, International Technology Roadmap for Photovoltaic 2022.
- 3. A. Louwen et al., Solar Energy Materials and Solar Cells **147**, 295–314 (2016).
- 4. Y. Zhang et al., Energy & Environmental Science **14**, 5587–5610 (2021).
- 5. J. Levrat et al., in Proceedings of the 42nd Photovoltaic Specialist Conference (PVSEC), 1–3 (2015).
- 6. A. Faes et al., in Proceedings of the 7th World Conference on Photovoltaic Energy Conversion (WCPEC), 1998–2001 (2018).
- 7. Atteq ur Rehman et al., Progress in Photovoltaics: Research and Applications (2021).
- 8. C. N. Kruse et al., Energy Procedia **124**, 84–90 (2017).
- 9. M. A. Green et al., Progress in Photovoltaics: Research and Applications **30**, 687–701 (2022).
- J. Hohl-Ebinger et al., in Proceedings of the 23rd European Photovoltaic Solar Energy Conference and Exhibition, 2012–2016 (2008).
- 11. R. Sinton, Presented at the 1st Bifi PV Workshop (2012).

- 12. K. Emery, Presented at the 43rd IEEE Photovoltaic Specialists Conference (2016).
- 13. I. Geisemeyer et al., in Proceedings of the 29th European Photovoltaic Solar Energy Conference and Exhibition, 1202–1207 (2014).
- 14. K. Bothe et al., in Proceedings of the 37th European Photovoltaic Solar Energy Conference and Exhibition, 277–281 (2020).
- 15. Y.-J. Huang et al., IEEE Journal of Photovoltaics, 1–5 (2021).